Clays and Clay Minerals, Vol. 57, No. 6, 795–807, 2009.

CARBONATE-INDUCED STRUCTURAL PERTURBATION OF Al HYDROXIDES

G. Y. Zhang[1,2], Y. F. Hu[3], R. K. Xu[1,4], J. J. Dynes[5,6,*], R. I. R. Blyth[3], L. M. Kozak[1], and P. M. Huang[1,†]

[1] Department of Soil Science, University of Saskatchewan, 51 Campus Drive, Saskatoon, SK, S7N 5A8, Canada
[2] Department of Resources and Environmental Science, Agricultural University of Hebei, Baoding, China
[3] Canadian Light Source, 101 Perimeter Road, Saskatoon, SK S7N 0X4, Canada
[4] Institute of Soil Science, Chinese Academy of Sciences, P.O. Box 821, Nanjing, China
[5] Environment Canada, 11 Innovation Boulevard, Saskatoon, SK, S7N 3H5, Canada
[6] Department of Chemistry, McMaster University, Hamilton, ON, L8S 4M1, Canada

Abstract—The chemistry of Al transformation has been well documented, though little is known about the mechanisms of structural perturbation of Al precipitates by carbonates at a molecular level. The purpose of the present study was to investigate the structural perturbation of Al precipitates formed under the influence of carbonates. Initial carbonate/Al molar ratios (MRs) used were 0, 0.1, and 0.5 after aging for 32 days, then the samples were analyzed by X-ray absorption near edge structure spectroscopy (XANES), X-ray diffraction (XRD), Fourier-transform infrared absorption spectroscopy (FTIR), and chemical analysis. The XRD data were in accord with the FTIR results, which revealed that as the carbonate/Al MR was increased from 0 to 0.1, carbonate preferentially retarded the formation of gibbsite and had relatively little effect on the formation of bayerite. As the carbonate/Al MR was increased to 0.5, however, the crystallization of both gibbsite and bayerite was completely inhibited. The impact of carbonate on the nature of Al precipitates was also evident in the increase of adsorbed water and inorganic C contents with increasing carbonate/Al MR. The Al K- and L- edge XANES data provide the first evidence illustrating the change in the coordination number of Al from 6-fold to mixed 6- and 4-fold coordination in the structural network of short-range ordered (SRO) Al precipitates formed under the increasing perturbation of carbonate. The fluorescence yield spectra of the O K-edge show that the intensity of the peak at 534.5 eV assigned to σ* transitions of Al−O and O−H bonding decreased with increasing carbonate/Al MR. The XANES data, along with the evidence from XRD, FTIR, and chemical analysis showed clearly that carbonate caused the alteration of the coordination nature of the Al−O bonding through perturbation of the atomic bonding and structural configuration of Al hydroxides by complexation with Al in the SRO network of Al precipitates. The surface reactivity of an Al−O bond is related to its covalency and coordination geometry. The present findings were, therefore, of fundamental significance in understanding the low-temperature geochemistry of Al and its impacts on the transformation, transport, and fate of nutrients and pollutants in the ecosystem.

Key Words—Al transformation, Carbonate, Complexation, Coordination Nature, Ecosystem, Short-range Ordered Mineral Colloids, Structural Disorder, XANES Spectroscopy.

INTRODUCTION

Aluminum hydroxides are ubiquitous in mineral soils, especially in tropical and sub-tropical soils. They are known to exist as crystalline and short-range ordered (SRO) mineral colloids which vary widely in terms of crystallinity and in their charge characteristics and surface properties, and likewise in their adsorption capacity for essential nutrients and environmental pollutants, including natural and synthetic molecules (Sposito, 1996; Huang *et al.*, 2002). As a result, the nature of the Al precipitates plays an important role in influencing the transformation and the transport of nutrients and pollutants in the environment (Violante *et al.*, 2002; Huang, 2004, 2008). Aluminum hydroxides have been used widely in industrial and environmental engineering (Tanada *et al.*, 2003; Ogata *et al.*, 2006; Cai *et al.*, 2008) and also in the pharmaceutical industry (Serna *et al.*, 1978a, 1978b; Levesque *et al.*, 2006; Hansen *et al.*, 2007).

The crystallinity of Al hydroxides as well as their chemical and physical properties are influenced significantly by pH and by the organic and inorganic anions present during their formation. Inorganic anions such as ClO_4^-, NO_3^-, and Cl^- do not influence the hydrolysis and polymerization of Al significantly when those anions are present at low concentrations (Hsu, 1967; Huang *et al.*, 2002), whereas SO_4^{2-}, PO_4^{3-}, SiO_4^{4-}, CO_3^{2-}, and F^- have a strong affinity for Al (Hsu, 1973, 1979; Violante and Huang, 1985; Bardossy and White, 1979; Huang *et al.*, 2002). Inorganic ligands with a strong affinity for Al can promote the formation of SRO Al hydroxides. The evidence obtained by infrared (IR) absorption spectroscopy (Serna *et al.*, 1977) revealed that carbonate is coordinated with the surface Al cations on Al hydroxide

* E-mail address of corresponding author:
james.dynes@usask.ca
† Deceased
DOI: 10.1346/CCMN.2009.05706012

https://doi.org/10.1346/CCMN.2009.05706012 Published online by Cambridge University Press

gels. Compared with NO_3^-, the interaction between the CO_3^{2-} and Al hydroxide gel appears to be strongest and to be responsible for the relatively high degree of stability of the carbonate-containing Al hydroxide gel (Serna *et al.*, 1977). The effects of the structure, functionality, and concentration of organic ligands on the crystallization of Al hydroxides have been investigated since the 1970s (Kwong and Huang, 1975, 1979; Violante and Huang, 1985; Colombo *et al.*, 2004; Yu *et al.*, 2007). The ability of organic acids to hamper crystallization of Al hydroxides is closely related to the ability of organic ligands to complex with Al ions. X-ray absorption spectroscopy (XAS) has shown that the coordination nature of Al hydroxides can be perturbed by organic acids such as tannic acid (Hu *et al.*, 2008). Little is known, however, about the coordination nature of Al hydroxides formed under the influence of inorganic ligands, such as carbonate.

Carbonate is a ligand, common in soil, water, and air, and it plays an important role in influencing the hydrolysis of Al (Serna *et al.*, 1977). However, only limited information is available on the interaction between carbonate and Al ions and the resulting influence on the crystallization of Al hydroxides (Serna *et al.*, 1977; Bardossy and White, 1979; Ma *et al.*, 2001). In agriculture, the liming of acid soils can neutralize the acidity and precipitate Al, thereby influencing the nature of the Al transformation products in soils. Soil properties related to the transformation of nutrients and pollutants could, thus, be affected by the application of lime.

Little is known about the mechanisms responsible for the structural perturbation, at a molecular level, of Al precipitation products by carbonate. Even less is known about the impact of carbonate-induced structural perturbation of the nanoscale surface properties of Al precipitates. The use of X-ray absorption spectroscopy (XAS) for structural characterization of Al precipitation products by carbonate is advantageous for several reasons. The technique provides information on the local chemical and structural environment and oxidation states of the element, and it makes possible the study of different edges of different elements of the same system for a more complete bonding picture. In addition, XANES is non-destructive, and depth information can be obtained when different detection modes are used. For example, the total electron yield (TEY) of the Al L-edge is very surface-sensitive with an estimated probing depth of 7 nm (Zou *et al.*, 1999); while the fluorescence yield (FLY) of the Al K-edge can probe much deeper with an estimated sampling depth of several hundreds of nm (Kasrai *et al.*, 1996; Zou *et al.*, 1999). The multi-element, multi-detection technique permits probing of different elements of the sample.

The objective of the study was to investigate the structural perturbation of Al hydroxides formed under the influence of carbonate. The interaction between carbonate and Al ions and the resulting impact on the nature of the Al hydroxides was studied further by XRD, FTIR, and XANES. The information obtained will increase understanding of the interaction mechanisms between carbonate and Al ions, and the role of carbonate in influencing the nature of the Al transformation products in the environment.

MATERIALS AND METHODS

Preparation of Al hydroxide precipitates

To synthesize Al hydroxide precipitates in the absence of carbonate, 1000 mL of 0.01 M $AlCl_3$ solution was titrated slowly with 0.1 M NaOH solution to pH 7.0 with constant stirring in a Glove Box filled with N_2. The suspension pH was kept at pH 7.0 for 30 min. The rate of addition of NaOH was ~2.5 mL min^{-1}. The synthesis of the Al hydroxide precipitates in the presence of carbonate [carbonate/Al molar ratios (MRs) of 0.1 and 0.5] was similar to the synthesis of the sample formed in the absence of carbonate. The 0.01 M $AlCl_3$ solution was titrated with 0.1 M NaOH until a suspension pH of 4.2−4.3 was reached, after which 10 mL and 50 mL of 0.1 M Na_2CO_3 solution were added to separate suspensions to adjust the carbonate/Al MRs to 0.1 and 0.5, respectively. Additional 0.1 M NaOH solution was then titrated into each suspension up to pH 7.0, a value maintained for 30 min. After aging for 2 days, the pH of all suspensions, both in the absence and presence of carbonate, was adjusted to maintain the pH at 7.0 by adding 0.1 M NaOH or HCl for 7 days. All the suspensions with initial carbonate/Al MRs of 0, 0.1, and 0.5 were aged for 32 days at room temperature (~23−25ºC). During aging, the suspensions were agitated once a day. At the end of the aging period, the suspensions were centrifuged at 16,080 g (Sorval RC5B, Mandel Scientific Co. Ltd.) for 10 min. The Al precipitates were washed once with 50% ethanol and then three or more times with 95% ethanol (with varying percentages of acetone if necessary to maintain flocculation) as needed. The suspensions were centrifuged at 36,182 g after each washing and 0.1 M $AgNO_3$ was used to test for chloride until the clear decantate was free of chloride. Once free of chloride the Al precipitates were air dried at room temperature.

Reference materials

The reference compounds included gibbsite [γ-$Al(OH)_3$], bayerite [α-$Al(OH)_3$], SRO Al hydroxides, $AlPO_4$, pseudoboehmite (γ-AlOOH), and γ-Al_2O_3. The gibbsite (research grade, synthetic) was obtained from Ward's Natural Science (Rochester, New York). Bayerite was synthesized according to the method described by Violante and Huang (1993). The SRO Al hydroxides were prepared according to Huang *et al.* (1977). The $AlPO_4$, obtained from Aldrich Chemical Company (Milwaukee, Wisconsin), was >99% pure. The

https://doi.org/10.1346/CCMN.2009.05706012 Published online by Cambridge University Press

pseudoboehmite was obtained from BASF Catalysts LLC (Iselin, New Jersey). The γ-Al_2O_3 was >99% pure and was obtained from Alfa Aesar (Ward Hill, Massachusetts). All the Al-containing minerals were verified by XRD.

The reference compounds were selected to represent compounds with known Al coordination numbers (CNs) of 4 and 6, and mixed CNs of 4 and 6; and they were considered to be relevant to the study of the synthesized samples. Specifically, gibbsite and bayerite have 6-fold coordination (Bragg and Claringbull, 1965) and they were present in the synthesized systems; $AlPO_4$ has 4-fold coordination (Berry and Mason, 1959); and γ-Al_2O_3 has both 4- and 6-fold coordination (Yoon *et al.*, 2004). Pseudoboehmite and SRO Al hydroxides were also selected as reference compounds for comparison.

Determination of inorganic C and adsorbed water contents

The total C and organic C contents of the Al precipitates were determined by the dry combustion of 0.2 g samples at 1100ºC and 840ºC, respectively, using the C632 Carbon Determinator (LECO Corporation, St. Joseph, Michigan) (Wang and Anderson, 1998). The inorganic C in the Al precipitates was determined from the difference between the total and organic C contents of the precipitates. The adsorbed water content of the air-dried precipitates was determined by heating samples at 110ºC for 24 h and measuring the loss of mass (Gardner, 1986). The adsorbed water and inorganic C contents are shown in Table 1.

XRD and FTIR analysis

50 mg of each Al precipitate was powder-mounted on a glass slide using several drops of acetone to make a slurry, dried, and analyzed by XRD with FeKα radiation generated at 40 kV and 160 mA using a Rigaku X-ray diffractometer (Rigaku Rotaflex Model RU-200, Tokyo) equipped with an incident-beam graphite monochromator. The XRD patterns were recorded from 4 to 60º2θ in steps of 0.02º2θ at a scanning rate of 10º2θ min^{-1} in continuous mode. The preparation of all the powder-mounted slides was conducted in the same manner.

The FTIR spectra of samples were recorded on an FTS-40 BIO-RAD Digilab Division instrument (Cambrige, Massachusetts) using the KBr pellet technique. The KBr pellets were prepared by mixing 1 mg of slightly ground sample with 200 mg of oven-dried (at 105−110ºC) KBr and then pressing the mixture into a disc. The FTIR spectra were scanned from 400 to 4000 cm^{-1} and were collected at a resolution of 4 cm^{-1}. The spectra were analyzed with BIO-RAD Win-IR™, Microsoft Windows 95, Version 4.14, Level II software.

XANES analysis

The XANES measurements were performed at the Canadian Light Source (Saskatoon, Canada), using the variable line spacing plane grating monochromator (PGM) and the spherical grating monochromator (SGM) beamlines. The PGM beamline provides photons between 5.5 and 250 eV (Hu *et al.*, 2007), and was used to study the Al L-edge. The SGM beamline, covering a photon range of 250−2000 eV (Regier *et al.*, 2007), was used to study the Al and O K-edges. The energy scale of the PGM was calibrated using sharp features in inert gases such as Xe and Kr (Hu *et al.*, 2007). Reference spectra of gibbsite, Si, and SiO_2 were used to calibrate the energy scale of the SGM (Ildefonse *et al.*, 1998; Hu *et al.*, 2004). The photon energy resolution values for Al L- and K-edge XANES were set to 0.1 and 0.6 eV, respectively. For O K-edge results, the photon energy resolution was set to 0.2 eV.

The fine powder of the Al precipitates and reference materials was spread on conducting, double-sided carbon tape and mounted on a stainless steel sample holder for obtaining Al L-edge, Al K-edge, and O K-edge spectra. The mounted sample was transferred through a load-lock stage into the main chamber for XANES measurement. Both surface-sensitive total electron yield (TEY) and the bulk sensitive fluorescence yield (FLY) were measured simultaneously. The TEY spectrum was recorded by monitoring the sample drain current directly. A micro-channel-plate detector was used to measure the FLY spectrum. All spectra were normalized against the beamline current measured by a Ni or Au mesh (90% transmission). An additional spline baseline was applied to the Al L-edge spectra due to distortions caused by sample charging and self-absorption. The apparent photon energy positions of the XANES features in the Al K- and L-edge and O K-edge spectra of the Al precipitates and reference materials were determined from the 2nd derivative (Table 2).

Table 1. Adsorbed water and inorganic carbon contents of the Al precipitates formed under the influence of carbonate.

Treatments	Adsorbed water (g/kg)	Inorganic carbon (g/kg)
Carbonate/Al MR* = 0	89.9±0.5	3.48±0.11
Carbonate/Al MR = 0.1	108.6±0.8	4.11±0.64
Carbonate/Al MR = 0.5	162.8±2.9	10.59±1.08

* Molar ratio

https://doi.org/10.1346/CCMN.2009.05706012 Published online by Cambridge University Press

Table 2. Apparent photon energy positions of the XANES features in the Al K- and L-edge, and O K-edge spectra of the Al precipitates and reference materials.

Samples	Energy position (eV)		
	Al K-edge TEY	Al L-edge FLY	O K-edge TEY and FLY
Gibbsite [γ-Al(OH)$_3$]	1567.7; 1570.7	77.7; 80.5	*532.2; 534.8; 540.5; 558.4 #532.0; 534.5; 540.1; 559.0
Pseudoboehmite [γ-AlOOH]	1567.6; 1570.8; 1571.4	78.8; 80.7	*532.1; 540.0; 559.0 #531.1; 539.7; 559.7
SRO Al hydroxides	1568.1; 1570.7	77.6; 80.5	*531.9; 539.8; 557.7 #531.9; 540.2; 559.0
$AlPO_4$	1565.8	78.4; 81.4	*532.1; 537.7; 558.5 #532.2; 537.7; 557.8
γ-Al_2O_3	1565.4; 1567.7; 1570.7; 1575.2	78.1; 79.9; 84.3	*532.1; 541.0; 559.0 #532.2; 540.7; 559.6
Bayerite [α-Al(OH)$_3$]	1567.7; 1570.7	77.4; 80.6; 84.5	*532.2; 540.3; 558.8 #535.1; 540.3; 559.0
Carbonate/Al MR[†]= 0	1567.2; 1570.2	77.7; 80.6	*540.4; 558.9 #534.7; 540.2;558.9
Carbonate/Al MR = 0.1	1567.2; 1570.2	77.6; 80.9	*531.1; 540.3; 558.5 #531.0;540.2; 559.0
Carbonate/Al MR = 0.5	1567.5; 1570.2	77.5; 81.2	*532.7; 540.2; 558.6 #540.0; 559.0

*TEY
FLY
[†] Molar ratio

RESULTS AND DISCUSSION

XRD patterns

The XRD patterns of the Al precipitation products formed under the influence of carbonate at carbonate/Al MRs of 0, 0.1, and 0.5 are shown in Figure 1. In the absence of carbonate (Figure 1a) and at a carbonate/Al MR of 0.1 (Figure 1b), the crystalline species identified in the Al precipitates after aging for 32 days were gibbsite and bayerite. As the carbonate/Al MR was increased from 0 to 0.1, the intensity of the gibbsite peaks at 4.81, 4.35, 3.30, 2.44, 2.38, and 2.04 Å decreased substantially. The presence of carbonate retarded gibbsite formation and increased the presence of SRO materials. The trend was not as clear, however, in the case of bayerite. The X-ray data indicate that the phase fraction of gibbsite in the two-phase mixture (the ratio of gibbsite to bayerite contents) was reduced as the carbonate/Al MR increased from 0 to 0.1.

For the Al precipitates formed at a carbonate/Al MR of 0.5, the crystallization of both gibbsite and bayerite was inhibited (Figure 1c). Carbonate has a strong affinity for Al (Bardossy and White, 1979; Huang *et al.*, 2002) and can be coordinated with the Al cation on Al hydroxide gels (Serna *et al.*, 1977; Feldkamp *et al.*, 1981). Aqueous solutions of Al ions are subject to extensive hydrolysis (Sposito, 1996; Huang *et al.*, 2002). In the absence of carbonate, the positively charged edges of the hydroxyl-Al polymers undergo hydrolysis. In the presence of carbonate in the aqueous solution of Al, the occupation of the coordination sites of Al by carbonate, instead of H_2O molecules, would impose a restraint on the hydrolysis of Al. The more carbonate that is added to the system, the greater would be the replacement of H_2O molecules by carbonate and subsequent blocking of the coordination sites of Al, resulting in a greater restraint on the subsequent hydrolysis of the hydroxyl-Al polymers. Carbonate ligands disrupt the hydroxyl-building mechanism which is essential for the formation of crystalline Al hydroxides. Furthermore, because of steric factors, the perturbing carbonate ligands occupying the coordination sites of Al hydroxides distort the unit sheets of Al hydroxides, leading to the formation of non-crystalline precipitation products of Al. The combination of these reaction processes would account for the inhibition of the formation of the crystalline Al hydroxides by carbonate (Figure 1c).

FTIR spectra

The FTIR spectra of Al precipitates formed at different initial carbonate/Al MRs of 0, 0.1, and 0.5 are shown in Figure 2. In the absence of carbonate (carbonate/Al MR = 0) (Figure 2a), the Al precipitates formed were a mixture

https://doi.org/10.1346/CCMN.2009.05706012 Published online by Cambridge University Press

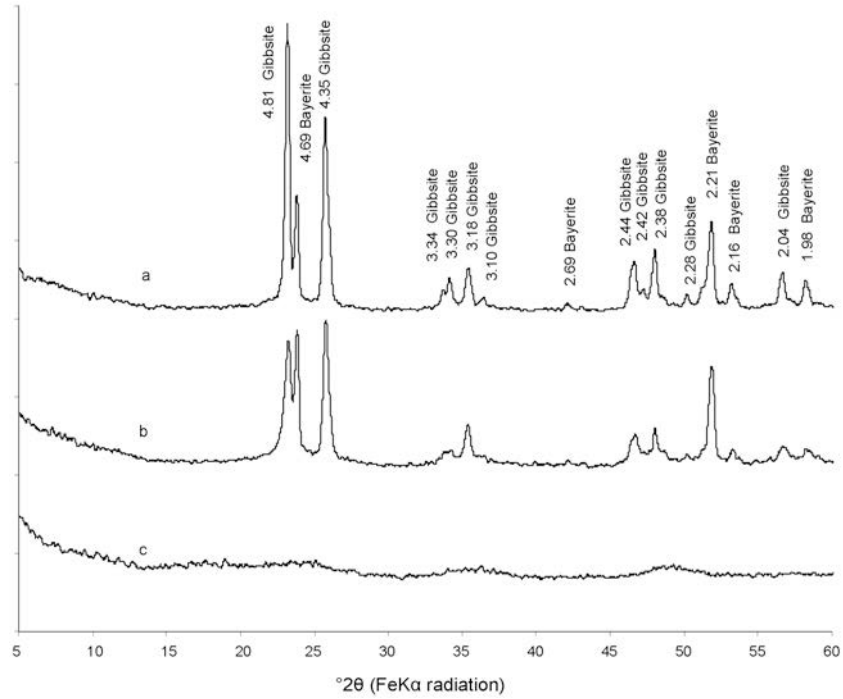


Figure 1. XRD patterns of the Al precipitates formed under the influence of carbonate at the initial carbonate/Al molar ratios (MRs): (a) 0, (b) 0.1, and (c) 0.5 after aging for 32 days. The *d* values are given in Å.

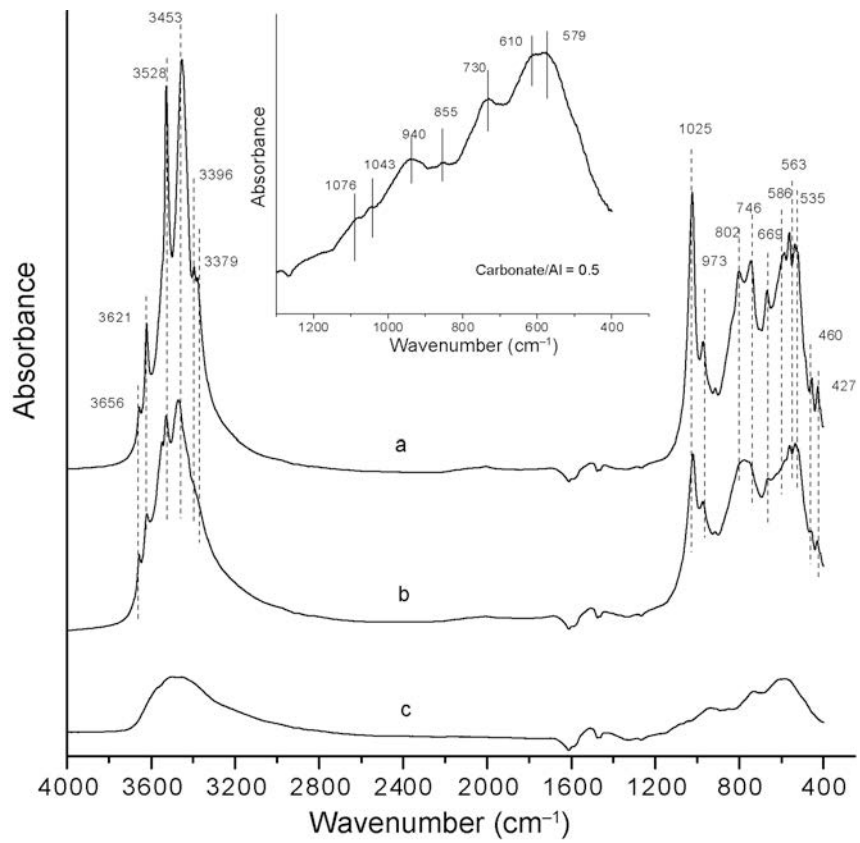


Figure 2. FTIR spectra of the Al precipitates formed under the influence of carbonate at initial carbonate/Al molar ratios (MRs) of: (a) 0, (b) 0.1, and (c) 0.5 after aging for 32 days. The inset provides an expanded view of the 1200−400 cm^{-1} portion of spectrum c.

https://doi.org/10.1346/CCMN.2009.05706012 Published online by Cambridge University Press

of bayerite (3656 cm^{-1}) and gibbsite (3621, 3528, 3453, 3396, 3379, 1025, 973, 802, 746, and 669 cm^{-1}) (van der Marel and Beutelspacher, 1976). The bands at 586, 563, 535, 460, and 427cm^{-1} can be ascribed to bayerite/gibbsite based on the characteristic bands of bayerite (586, 560, 531, 460, and 428 cm^{-1}) and gibbsite (590, 560, 533, 453, and 423−430 cm^{-1}) (van der Marel and Beutelspacher, 1976). The FTIR results of the carbonate/Al MR = 0 sample (Figure 2a) were in agreement with the XRD (Figure 1a).

The FTIR spectrum of the Al precipitates formed at a carbonate/Al MR of 0.1 (Figure 2b) shows nearly the same bands as those present in the precipitates formed at the carbonate/Al MR of 0 (Figure 2a). The spectrum (Figure 2b) also shows the presence of a mixture of bayerite (3656 cm^{-1}) and gibbsite (3620, 3548, 3528, 3476, 1021, 974, and 663 cm^{-1}). The bands at 587, 561, 534, 460, and 427 cm^{-1} are attributed to bayerite/gibbsite. Compared with the Al precipitate formed at the carbonate/Al MR = 0, however, the bands at 3396 and 3379 cm^{-1} were virtually absent and the bands at 802 and 746 cm^{-1} merged, resulting in a broad band at ~779 cm^{-1} in the Al precipitates formed at the carbonate/Al MR of 0.1. In addition, the band at 586 cm^{-1} in the spectrum of the Al precipitates formed at the carbonate/Al MR = 0 was reduced to a small shoulder in the spectrum of the Al precipitate formed at the carbonate/Al MR of 0.1.

As the initial carbonate/Al MR was increased to 0.5 (Figure 2c), the absorption bands characteristic of the crystalline Al hydroxides virtually disappeared. From 3700−3300 cm^{-1}, a single broad band was observed, which was attributed to the formation of poorly crystalline Al precipitates resulting from the influence of carbonate at a carbonate/Al MR = 0.5. The FTIR data of the Al precipitates formed under the influence of carbonate (Figure 2) support their XRD data (Figure 1), corroborating the complexation of Al with carbonate and the resultant structural perturbation of the Al precipitate formed. The extent of the perturbation increased with increase in the carbonate/Al MR.

The bands at 1076, 1043, 940, 855, 730, 610, and 579 cm^{-1} in the inset (the spectrum of 400−1200 cm^{-1}) of Figure 2c clearly show the presence of carbonate (White, 1974; van der Marel and Beutelspacher, 1976). The FTIR data illustrate, therefore, that carbonate was co-precipitated with Al in the precipitates formed at a carbonate/Al MR of 0.5 (Figure 2c). The carbonate absorption bands were not present in the Al precipitates formed at carbonate/Al MRs of 0 and 0.1.

Adsorbed water and inorganic carbon contents

The adsorbed water contents of the Al precipitates increased substantially with increasing initial carbonate/Al MRs (Table 1). The adsorbed water content of the precipitates formed at the carbonate/Al MR of 0.5 was 1.8 times greater than that of the precipitates formed at the carbonate/Al MR of 0, attributed to the carbonate-induced structural perturbation of the Al precipitates (Figures 1, 2), which apparently promoted the penetration of polar water molecules into the short-range ordered structural network and the subsequent coordination of water molecules with the Al in the carbonate-containing Al precipitates. Yu *et al*. (2007) also reported that the adsorbed water content of the Al precipitates increases with increasing tannate/Al MR by promoting the penetration of water molecules into the poorly crystalline to non-crystalline particles and coordination of water molecules to the tannate-Al complexes.

The inorganic C content of the Al precipitates also increased with increasing carbonate/Al MR (Table 1). At the carbonate/Al MR = 0, the inorganic C (carbonate) present in the Al precipitates was attributable to the presence of inorganic C as an impurity. As the initial carbonate/Al MR increased from 0 to 0.5, the inorganic C increased by a factor of 3 (Table 1), resulting in the structural perturbation and formation of non-crystalline Al precipitates by complexation of Al with carbonate (Figures 1, 2) and also in the substantial increase in the adsorbed water (Table 1). The data indicate the increasing hindering effect of carbonate on the crystallization of Al hydroxide through incorporation of carbonate and water molecules in the structural network with increasing carbonate/Al MR. The XRD and FTIR data indicate no similarity between this amorphous phase (Figures 1c, 2c) and scarbroite/hydroscarbroite, which are crystalline (International Centre for Diffraction Data, 2007) and have distinct IR spectra (White, 1974).

Al K-edge

Aluminum K-edge XANES is a powerful tool for probing atomistic-level information (Doyle *et al.*, 1999; Fenter *et al.*, 2002) and has been used to explore the bonding and symmetry of the local environment around Al atoms and to differentiate between 6-fold (CN = 6) and 4-fold coordination (CN = 4) for Al atoms (Li *et al.*, 1995; Ildefonse *et al.*, 1998; Doyle *et al.*, 1999; Van Bokhover *et al.*, 1999). As reported previously (Hu *et al.*, 2008), the spectra of Al compounds with CN = 6 (*e.g.* gibbsite and boehmite) generally yield two main maxima at 1567.7±0.3 eV and 1571.5±0.4 eV (for boehmite, the second maximum splits into two). More specifically, the XANES spectrum of boehmite yields one edge maximum at 1567.6 eV (the greatest amplitude), two resonances with lesser amplitude at 1570.2 and 1571.6 eV (they were split from one maximum), and a shoulder resolved at greater energy at 1575 eV (Ildefonse *et al.*, 1998). The mean distance of the Al^{VI}−O bond is ~1.9 Å (Kato *et al.*, 2001).

The spectra of Al compounds (*e.g.* $AlPO_4$) with CN = 4 consist of a strong single-edge maximum at 1566.2±0.7 and four ill-defined features at greater energy (Ildefonse *et al.*, 1998; Hu *et al.*, 2008). The mean Al^{IV}−O distance is ~1.7 Å. The Al compounds

https://doi.org/10.1346/CCMN.2009.05706012 Published online by Cambridge University Press

with mixed CN = 4 and 6 (*e.g.* γ-Al_2O_3) yield three main maxima at 1566.2±0.2, 1567.4±0.5, and 1570.6±0.3 eV (Ildefonse *et al.*, 1998; Chaplais *et al.*, 2001; Hu *et al.*, 2008). The variations in spectral features, such as the overall peak position and shape, of the Al K-edge spectra of Al minerals with the same coordination number are related to the number of their Al sites, the distribution of Al−O distances, and the influence of the second neighbor.

The Al K-edge TEY spectra of the Al precipitates formed under the influence of carbonate and of the reference materials (gibbsite, bayerite, pseudoboehmite, SRO Al hydroxides, $AlPO_4$, and γ-Al_2O_3) are shown in Figure 3a. The FLY spectra were similar to the TEY spectra and so only the latter spectra are shown. The spectra of reference materials, such as gibbsite, $AlPO_4$, and γ-Al_2O_3 in the present study are in good agreement with previous reports (Ildefonse *et al.*, 1998; Doyle *et al.*, 1999; Yoon *et al.*, 2004). The present bayerite spectrum is slightly different from that of bayerite reported by Yoon *et al.* (2004). Peaks b at 1567.7 eV and c at 1570.7 eV of bayerite in the present study are better resolved than those of the bayerite from Yoon *et al.* (2004). Compared with gibbsite, peak b was more intense in bayerite (Figure 3a). The Al K-edge spectra of pseudoboehmite and SRO Al hydroxides (Figure 3a) are comparable to those from previous studies (Hu *et al.*, 2008). Compared with the Al K-edge spectrum of the boehmite from Ildefonse *et al.* (1998), the two peaks at 1570.8 and 1571.4 eV of pseudoboehmite are less well resolved (Figure 3a) than those of boehmite.

The Al K-edge spectrum of the Al precipitates formed at the carbonate/Al MR = 0 was similar to that of gibbsite, but different from SRO Al hydroxides and pseudoboehmite (Figure 3a). The relative intensity of peaks b and c of the precipitates formed at the carbonate/Al MR = 0 was between those of gibbsite and bayerite. The photon energy position of the two peaks (the Al precipitates) indicates that the Al was in 6-fold coordination. The XRD pattern and FTIR spectrum (Figures 1 and 2) also reveal that the Al precipitates formed were a mixture of gibbsite [γ-$Al(OH)_3$] and bayerite [α-$Al(OH)_3$]. The Al K-edge spectrum is, therefore, in accord with the XRD and FTIR results (Figures 1 and 2) obtained during the present work.

At the initial carbonate/Al MR of 0.1, the Al K-edge spectrum of the Al precipitate was very similar to the spectrum of the carbonate/Al MR = 0 precipitates (Figure 3a), except the intensity of peak b increased slightly relative to peak c, compared with the carbonate/Al MR = 0 (Figure 3a). Furthermore, a weak shoulder around 1566 eV became more apparent in the spectrum of the precipitates formed at an initial carbonate/Al MR = 0.1, which was not observed in the spectra of gibbsite and bayerite, but was distinctly evident in the spectrum of the SRO Al hydroxides (Figure 3a). The shoulder overlaps with the photon energy position of peak a, indicating the presence of some tetrahedral Al in the SRO Al hydroxides in the precipitates formed at a carbonate/Al MR of 0.1. The XRD and FTIR data (Figures 1b, 2b) show that gibbsite and bayerite were formed in the carbonate/Al MR = 0.1 system. However, carbonate preferentially hampered the formation of gibbsite over bayerite as indicated by the decrease in

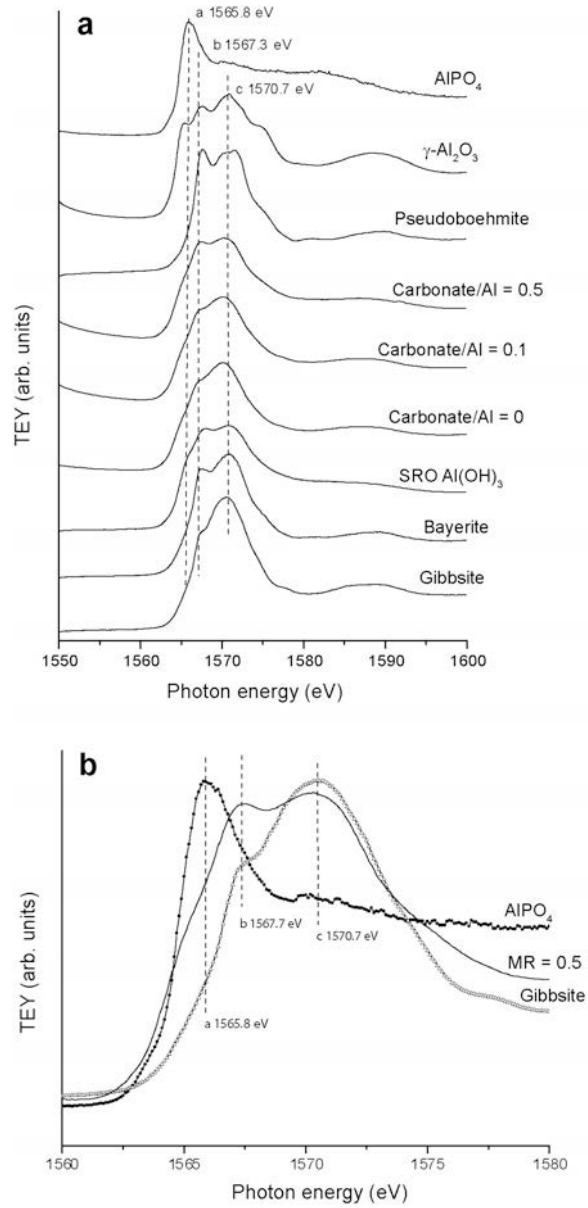


Figure 3. Al K-edge spectra (TEY) of: (a) the Al precipitates formed under the influence of carbonate at initial carbonate/Al molar ratios (MRs) of 0, 0.1, and 0.5 after aging for 32 days and the reference materials gibbsite, bayerite, SRO $Al(OH)_3$, pseudoboehmite, γ-Al_2O_3, and $AlPO_4$; (b) the expanded photon energy and intensity scales in the range of 1560−1580 eV for the spectra of the Al precipitate formed at a carbonate/Al MR = 0.5, gibbsite, and $AlPO_4$.

https://doi.org/10.1346/CCMN.2009.05706012 Published online by Cambridge University Press

the intensity and/or the increase in the broadening of the XRD peaks and FTIR absorption bands of gibbsite (Figures 1a, 1b, 2a, and 2b). The reduced formation of gibbsite was attributed to the coordination of carbonate with Al, resulting in the formation of less ordered gibbsite particles and some SRO Al hydroxide precipitates (Figure 3a).

As the carbonate/Al MR was increased from 0.1 to 0.5, the energy positions of peaks b and c remained unchanged (Figure 3a,b), indicating that the Al in the precipitates was still largely 6-fold coordinated (Figure 3b). The weak shoulder at 1566 eV became a little more distinct, although a similar but more pronounced shoulder was also observed in the spectrum of SRO $Al(OH)_3$ (Figure 3a) and its energy position (1566 eV) was very close to the single-maximum peak (1565.8 eV) of $AlPO_4$ (Figure 3b), indicating the presence of some 4-fold coordinated Al in the precipitates. The intensity of peak b increased to almost the same intensity as that of peak c in the carbonate/Al MR = 0.5 precipitates. Its spectral shape and the relative intensity of peaks b and c were basically the same as those of the SRO $Al(OH)_3$ (Figure 3a), indicating a strong structural perturbation of Al hydroxides by carbonate at this carbonate/Al MR. Data from XRD and FTIR (Figures 1c and 2c) support this and show that the precipitates were non-crystalline materials. A similar trend of changes in the spectral shape and relative peak intensity of the Al precipitates formed under the influence of tannic acid was observed by Hu *et al.* (2008) who reported a change in coordination number of Al from 6-fold to mixed 6- and 4-fold coordination in the structural network of the SRO Al hydroxides formed under the increasing perturbation of tannic acid. The Al K-edge spectrum of the precipitates, formed at a carbonate/Al MR of 0.5, was different from that of pseudoboehmite (Figure 3a) and boehmite (Ildefonse *et al.*, 1998), as the intensity of peak b was greater than that of peak c in boehmite/pseudoboehmite, and peak c in boehmite/pseudoboehmite tended to split into two peaks. The XRD data do not provide unequivocal evidence that the Al oxyhydroxides were present in the carbonate/Al MR = 0.5 precipitates (Figure 1c).

The results (Figures 1–3) indicate that carbonate greatly perturbed the formation of Al hydroxides and altered the coordination geometry of Al. With increasing carbonate/Al MR, the formation of the Al hydroxides was increasingly retarded and the coordination nature of Al was increasingly altered as more of the Al was complexed with carbonate. The fact that no difference was observed between the FLY and TEY spectra of the Al K-edge indicates that perturbation of the crystallization of Al hydroxides by carbonate and the alteration of the coordination nature of Al not only occurred at the surface, but also extended throughout the structural network of the Al precipitates formed under the influence of carbonate.

Al L-edge

The Al L-edge has not been used as widely as the Al K-edge to investigate the bonding and symmetry of the local environment around Al atoms. Several electron energy loss spectroscopy studies of Al L-edge, particularly in the near edge (ELNES, electron loss near edge structure), have been conducted, however, to study the structural and chemical properties of Al-bearing samples (Jiang *et al.*, 2002; Bouchet and Colliex, 2003). Compared with the Al K-edge, the Al L-edge should be more sensitive to the chemical environment, such as ligand type, namely, the second neighbor (Stohr, 1992).

The Al L-edge FLY XANES spectra of Al precipitates formed at carbonate/Al MRs of 0, 0.1, and 0.5 and the reference materials are shown in Figure 4. The Al L-edge spectra of different types of Al oxides and $AlPO_4$ using ELNES were reported by Jiang *et al.* (2002) and Bouchet and Colliex (2003), and using XANES by Chen *et al.* (1993), Hu *et al*. (2008), and Weigel *et al.* (2008). The first transition in the Al L-edge for crystalline minerals is usually split into two peaks with a separation of 0.45 eV [*e.g.* α-Al_2O_3 (Chen *et al.*, 1993) and $AlPO_4$

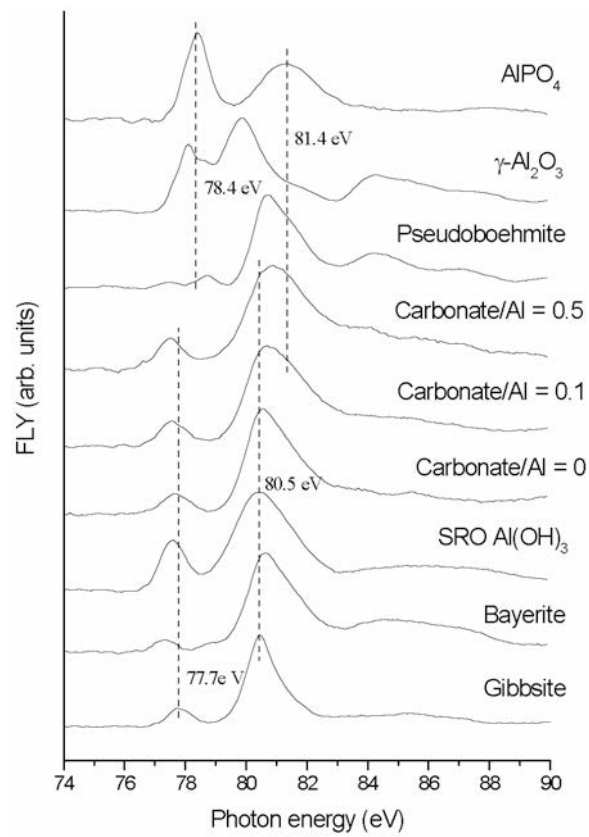


Figure 4. Al L-edge spectra (FLY) of the Al precipitates formed under the influence of carbonate at initial carbonate/Al molar ratios (MRs) of 0, 0.1, and 0.5 after aging for 32 days and the reference materials gibbsite, bayerite, SRO $Al(OH)_3$, pseudoboehmite, γ-Al_2O_3, and $AlPO_4$.

https://doi.org/10.1346/CCMN.2009.05706012 Published online by Cambridge University Press

(Weigel *et al.*, 2008)]. The second peak was observed at greater energy, ~80 eV. The energy position of the Al L-edge XANES is sensitive to the local bonding environment of Al sites. Mixed peaks could be resolved if Al existed in more than one coordination site (*e.g.* γ-Al_2O_3, Figure 4). In the case of $AlPO_4$, instead of two resolved L_3 and L_2 peaks at 77.9 and 78.3 eV (Weigel *et al.*, 2008), the spectrum of $AlPO_4$ in the present study (Figure 4) has only one broad peak at 78.4 eV, attributed to the amorphous nature of the $AlPO_4$ used in this study as verified by XRD and also noted by Hu *et al*. (2008).

For gibbsite, two peaks were evident, with the maximum at 80.5 eV being the more intense compared with the peak maximum at 77.7 eV (Figure 4). In the case of bayerite, the most intense peak was at 80.6 eV and the weakest peak was at 77.4 eV. The peak position of pseudoboehmite shifted to higher energy compared with gibbsite and bayerite. For SRO Al hydroxides, the stronger peak was at 80.5 eV and the weaker peak was at 77.6 eV. The Al L-edge spectrum of the Al precipitate formed at the carbonate/Al MR of 0 was basically the same as that of gibbsite (Figure 4). Its first peak (77.7 eV) was weaker, and the second peak (80.5 eV) was shifted only by 0.1 eV to a higher energy and substantially weaker and broader, compared with that of gibbsite. The shape and photon energy position of the second peak, however, looks the same as that of bayerite, attributed to the presence of both gibbsite and bayerite in the Al precipitate formed at the carbonate/Al MR = 0 as shown by the XRD (Figure 1a) and FTIR (Figure 2a) data.

The peak position and shape of Al L-edge spectrum of Al precipitates formed at a carbonate/Al MR = 0.1 were different, compared with those of the spectrum of Al precipitates formed at the carbonate/Al MR = 0 (Figure 4). Its first peak at 77.7 eV shifted to lower energy by 0.1 eV (77.6 eV), which was the same as that of SRO $Al(OH)_3$, whereas the second peak shifted to the higher-energy position by 0.3 eV (80.9 eV) in the carbonate/Al MR = 0.1 system compared to the precipitate formed at the carbonate/Al MR = 0 system. When the carbonate/Al MR was increased to 0.5, the first peak in the spectrum of Al precipitates formed shifted to a lower-energy position (77.5 eV) by 0.2 eV, and the second peak shifted by 0.6 eV to 81.2 eV. The peak at 81.2 eV for the carbonate/Al MR = 0.5 system was much broader than the same peak at the carbonate/Al MR = 0 and 0.1 (Figure 4). The data for Al L-edge indicate that carbonate perturbed the formation of Al hydroxides and, as a result, carbonate-containing, poorly ordered materials increased with the increasing carbonate/Al MR. The XRD (Figure 1) and FTIR (Figure 2) data revealed the same trend. Furthermore, the increase of the shift in energy position of the second peak to a higher-energy value with the increasing carbonate/Al MR is ascribed to the effect of the second neighbor of Al, *i.e.* Al-O-C and Al-O-Al. Besides the Al coordination, the edge position is also affected by the covalency of the bond which is, in turn, influenced by the bonding of Al−O to Al or C. According to the Pauling electronegativity scale, the values of C and Al are 2.5 and 1.5, respectively (Evans, 1966; Daintith, 1990). The ability of the C atom to gain electrons is thus greater than that of Al. More energy is, therefore, required to excite the electrons and dissociate the bond in Al-O-C than in Al-O-Al, which accounts for the shift in energy position of the second peak to a higher-energy position in the Al precipitates formed at greater carbonate/Al MRs. Furthermore, the photon energy position of the second peak at 81.2 eV of the Al precipitates formed at a carbonate/Al MR = 0.5 was very close to that of the second peak at 81.4 eV of the $AlPO_4$. The data (Figure 4) strongly indicate that besides the 6-fold coordinated Al, the presence of which was proved by the presence of the peak at 77.5 eV, the carbonate-perturbed Al precipitates formed at the carbonate/Al MR = 0.5 also contained some 4-fold coordinated Al.

O K-edge

The O K-edge spectra are sensitive to the nature of the element to which the O is bound rather than only to the O environment itself. Besides the early O K-edge XANES work of the 3d transition-metal oxides (de Groot *et al*., 1989), ELNES and XANES have been applied to investigate the O K-edge spectra of complex oxides (Bouchet and Colliex, 2003; Gilbert *et al*., 2003; Wang and Henderson, 2004; Jiang and Spence, 2006). Furthermore, Carbaret *et al*. (2007) recently used first-principles calculations to interpret O K-edge XANES data of germanates. Therefore, the O K-edge absorption may be used to probe orbital energies of metal−O bonds.

The O K-edge TEY and FLY spectra of Al precipitates formed at different carbonate/Al MRs and reference materials are shown in Figure 5a,b. Peak a at ~532.2 eV was observed in spectra of most of the reference materials, though it was weak in some (Figure 5a,b); it was most intense in the FLY spectrum of SRO $Al(OH)_3$. A peak at ~531.1 eV was present in the FLY and TEY spectra of pseudoboehmite. Peak a, at ~532.2 eV (very weak), was also present in the Al precipitates formed at carbonate/Al MRs of 0 and 0.5. A peak at 531.1 eV was observed in the carbonate/Al MR = 0.1 precipitate. The peaks might have been caused by contamination by carbon tape used for sample mounting and/or sorbed O_2 (Stohr, 1992) as well as beam damage. A weak pre-edge peak due to the radiation damage was also observed at 528.3 eV (Jiang and Spence, 2006) and 531 eV in the ELNES studies of Al oxides (Bouchet and Colliex, 2003). Compared to the previous XANES study, the beam damage merits special attention in the present study because more powerful, insertion device-based beamlines from a third-generation ring were used.

Peak b at 534.8 eV in Figure 5a was observed in the spectrum of gibbsite but was not evident in that of

https://doi.org/10.1346/CCMN.2009.05706012 Published online by Cambridge University Press

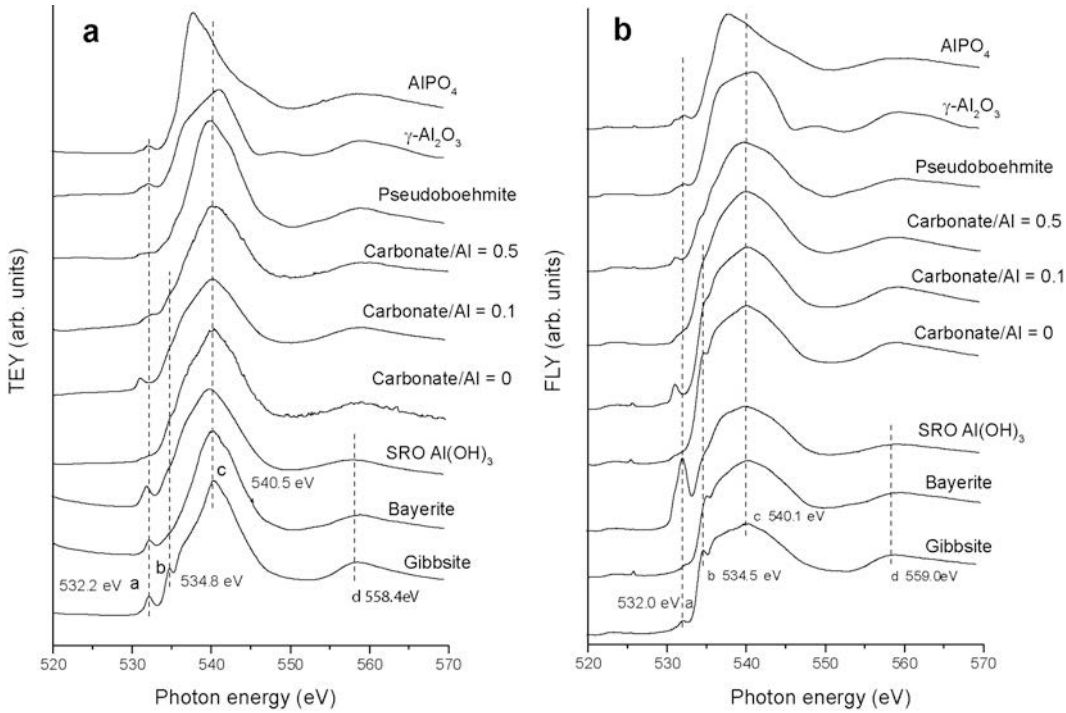


Figure 5. O K-edge spectra of the Al precipitates formed under the influence of carbonate at initial carbonate/Al molar ratios (MRs) of 0, 0.1, and 0.5 after aging for 32 days and the reference materials gibbsite, bayerite, SRO $Al(OH)_3$, pseudoboehmite, γ-Al_2O_3, and $AlPO_4$: (a) the TEY spectra, and (b) the FLY spectra.

bayerite; very weak shoulders around this energy position were observed in the spectra of SRO Al (oxyhydr)oxides, pseudoboehmite, as well as the three Al precipitates formed at the three different carbonate/Al MRs. Very strong and broad peaks at ~540.5 eV (peak c) were present in the spectra of the three Al precipitates formed at the carbonate/Al MRs of 0, 0.1, and 0.5 and some reference materials, except for γ-Al_2O_3 and $AlPO_4$ which had strong peaks at 541.0 and 537.7 eV, respectively. The peaks at ~540.5 eV and those at ~534.8 eV, including weak shoulders in this energy range, can be assigned to σ^* transitions of Al–O and O–H bonding (Bouchet and Colliex, 2003; Cabaret *et al*., 2007). σ^* bonding is the type of bonding in which O can be involved. The energy positions of peak c of the Al precipitates formed at the three carbonate/Al MRs were basically the same as those of the gibbsite, bayerite, SRO $Al(OH)_3$, and pseudoboehmite. Compared to gibbsite and bayerite, peak d of the SRO $Al(OH)_3$ was less intense. As the carbonate/Al MR increased from 0 to 0.5, the intensity of peak d also decreased, indicating the increasing perturbation effect of carbonate on the crystallization of Al hydroxides.

Distinct differences exist between the TEY and FLY spectra (Figure 5a,b). Previous studies reported that the penetrating depth of the TEY of the O K-edge was ~10–20 nm, whereas, that of the FLY is about an order of magnitude deeper (Henke *et al*., 1982; Hu *et al*., 2004). For the O K-edge spectra of gibbsite, bayerite, SRO Al hydroxides, pseudoboehmite, and the Al precipitates formed in the carbonate/Al MR of 0, 0.1, and 0.5 systems, peak c was broader in the FLY (Figure 5b) than in the TEY (Figure 5a), and the relative intensity of peak b was greater in the FLY than in the TEY. Peak b was evident in the O K-edge FLY spectrum of bayerite, but not in its TEY spectrum. Gibbsite has a very irregular structure with an average Al–O bond length of 1.924 Å, but with bond lengths of as little as 1.81 Å and as long as 2.09 Å (Thomas and Sherwood, 1992). Bulk gibbsite and the surfaces of gibbsite have been reported to differ in their structural and electronic properties and much more variability exists at depth *vs.* the surface (Frenzel *et al*., 2005). The O K-edge data (*e.g.* the shape of peak c in Figure 5a,b), therefore, support the reasoning that, at depth, considerably more variability is found in the gibbsite structure than on its surface. Peak b of gibbsite and bayerite was evident; but, in contrast, only a shoulder was observed in this energy region for the SRO $Al(OH)_3$ and pseudoboehmite (Figure 5b).

For the Al precipitates from the three carbonate/Al systems, peak b became less intense as the carbonate/Al MR increased from 0 to 0.1 to 0.5 (Figure 5b). The spectrum from the carbonate/Al MR = 0 system was basically the same as those of gibbsite and bayerite. When the carbonate/Al MR increased to 0.5, peak b

https://doi.org/10.1346/CCMN.2009.05706012 Published online by Cambridge University Press

disappeared and only a very small shoulder was observed. Peak d of the Al precipitates formed also decreased in intensity with increasing carbonate/Al MR. The results from the O K-edge FLY and TEY spectral analyses (Figure 5a,b) are in agreement with the XRD and FTIR data (Figures 1 and 2), indicating the structural disorder of Al precipitates caused by carbonate perturbation. Furthermore, the O K-edge spectroscopic data provided cutting-edge information on the role of carbonate in influencing the nature of Al precipitates formed at the molecular scale.

CONCLUSIONS

The chemistry of the transformation of Al as influenced by perturbing organic and inorganic ligands has been studied extensively (Kwong and Huang, 1975, 1978; Serna *et al*. 1977; Bardossy and White, 1979; Huang *et al*., 2002; Violante *et al*., 2002; Colombo *et al*., 2004; Yu *et al*., 2007). The coordination nature of Al (oxy)hydroxides, formed under the influence of tannic acid, and studied by XAS, was reported by Hu *et al*. (2008). Carbonate-induced structural perturbation at a molecular level, however, and the coordination nature of Al precipitation products, in particular, are yet to be elucidated.

Carbonate is a ligand which exists in the environment. The data obtained in the present study provide the first evidence showing the change of the coordination number of Al from 6-fold to mixed 6- and 4-fold coordination in the structural network of SRO Al precipitates formed under the increasing perturbation of carbonate. The adjustment of the coordination number of Al in the Al precipitates is attributed to steric and electronic factors, because Al is complexed with carbonate which has different functional groups and is larger in size than OH and H_2O. The Al K- and L-edge and O K-edge spectra of the Al precipitates, together with evidence from XRD, FTIR, and chemical analysis, demonstrated clearly that carbonate strongly perturbed the structural network of Al hydroxides by complexation with Al in the structural network of the SRO Al precipitates, which brought about a change in the coordination nature of the Al–O bonding.

The coordination structure of Al in Al precipitation products is of fundamental significance in understanding their atomic bonding and structural configuration and the influence on their surface chemistry at the molecular level, because the surface reactivity of a metal–O bond is related to the covalency and coordination geometry. The chemistry of the polynucleus complexes of Al could help to answer many questions about reactions at mineral surfaces (Casey *et al*., 2001; Hu *et al*., 2008). The present findings, therefore, have shed new light on the low-temperature geochemistry of Al, which merits attention by those regulating ecosystem health.

ACKNOWLEDGMENTS

This study was funded by Discovery Grant 2383-2008 of the Natural Sciences and Engineering Research Council of Canada. The XANES research work was performed at the Canadian Light Source (CLS), which was supported by NSERC, NRC, CIHR, and the University of Saskatchewan. The authors thank the CLS staff for their operation of the ring and help with PGM and SGM beamlines. Contributions by D. Peak, A. Hardie, R. de Freitas, and A. Seib are also much appreciated.

REFERENCES

Bardossy, G. and White, J.L. (1979) Carbonate inhibits the crystallization of aluminum hydroxide in bauxite. *Science*, **203**, 355–356.

Berry, L.G. and Mason, B. (1959) *Mineralogy.* W.H. Freeman and Company, San Francisco, CA, USA.

Bouchet, D. and Colliex, C. (2003) Experimental study of ELNES at grain boundaries in alumina: intergranular radiation damage effects on Al-$L_{2,3}$ and O-K edges. *Ultramicroscopy*, **96**, 139–152.

Bragg, L. and Claringbull, G.F. (1965) *Crystal Structures of Minerals.* G. Bell and Sons Ltd., London, UK.

Cabaret, D., Mauri, F., and Henderson, G.S. (2007) Oxygen K-edge XANES of germanates investigated using first-principles calculations. *Physical Review B*, **75,** 184205 (1–9).

Cai, Z.X., Kim, J.S., and Benjamin, M.M. (2008) NOM removal by adsorption and membrane filtration using heated aluminum oxide particles. *Environmental Science & Technology*, **42**, 619–623.

Casey, W.H., Phillips, B.L., and Furren, G. (2001) Aqueous aluminum polynuclear complexes and nanoclusters: A rewiew. Pp. 167–190 in: *Nanoparticles and the Environment* (J.F. Banfield and A. Navrotsky, editors). Reviews in Mineralogy and Geochemistry, **44**. The Mineralogical Society of America, Chantilly, VA, and Geochemical Society, St. Louis, MO.

Chaplais, G., Prouzet, E., Flank, A.-M., and Le Bideau, J. (2001) ^{27}Al MAS NMR and XAS cross-study of the aluminophosphonate Al(OH)($O_3PC_6H_5$). *New Journal of Chemistry*, **25**, 1365–1367.

Chen, J.M., Simons, J.K., Tan, K.H., and Rosenberg, R.A. (1993) Correlation between interatomic distances and the X-ray-absorption near-edge structure of single-crystal sapphire. *Physical Review* B, **48**, 10047–10051.

Colombo, C., Ricciardella, M., Cerce, A.D., Maiuro, L., and Violante, A. (2004) Effects of tannate, pH, sample preparation, aging and temperature on the formation and nature of Al oxyhydroxides. *Clays and Clay Minerals*, **52**, 721–733.

Daintith, J. (1990) *A Concise Dictionary of Chemistry.* Oxford University Press, Oxford, UK.

de Groot, F.M., Grioni, M.F., Fuggle, J.C., Ghijsen, J., Sawatzky, G.A., and Petersen, H. (1989) Oxygen 1s X-ray absorption edges of transition-metal oxides. *Physical Review B*, **40**, 5715–5723.

Doyle, C.S., Traina, S.J., Ruppert, H., Kendelewicz, T., Rehr, J.J., and Brown, G.E. Jr. (1999) XANES studies at the Al K-edge of aluminum-rich surface phase in the soil environment. *Journal of Synchrotron Radiation*, **6**, 621–623.

Evans, R.C. (1966) *An Introduction to Crystal Chemistry* 2nd edition. Cambridge University Press, London.

Feldkamp, J.R., Shah, D.N., Meyer, S.L., White, J.L., and Hem, S.L. (1981) Effect of adsorbed carbonate on surface charge characteristics and physical properties of aluminum hydroxide gel. *Journal of Pharmaceutical Sciences*, **70**, 638–640.

https://doi.org/10.1346/CCMN.2009.05706012 Published online by Cambridge University Press

Fenter, P.A., Rivers, M.L., Sturchio, N.C., and Sutton, S.R. (editors) (2002) *Applications of Synchrotron Radiation in Low-Temperature Geochemistry and Environmental Science.* Reviews in Mineralogy & Geochemistry, vol. **49**. The Mineralogical Society of America, Chantilly, VA, and Geochemical Society, St. Louis, MO.

Frenzel, J., Oliveira, A.F., Duarte, H.A., Heine, T., and Seifert, G. (2005) Structural and electronic properties of bulk gibbsite and gibbsite surfaces. *Zeitschrift für Anorganische Und Allgemeine Chemie*, **631**, 1267–1271.

Gardner, W.H. (1986) Water content. Pp. 493–544 in: *Methods of Soil Analysis, Part 1. Physical and Mineralogical Methods*, 2nd edition (A. Klute, editor). Agronomy Monograph no. **9**. Soil Science Society of America and American Society of Agronomy, Madison, Wisconsin.

Gilbert, B., Frazer, B.H., Belz, A., Conrad, P.G., Nealson, K.H., Haskel, D., Lang, J.C., Srajer, G., and De Stasio, G. (2003) Multiple scattering calculations of bonding and X-ray absorption spectroscopy of manganese oxides. *Journal of Physical Chemistry A*, **107**, 2839–2847.

Hansen, B., Sokolovska, A., HogenEsch, H., and Hem, S.L. (2007) Relationship between the strength of antigen adsorption to an aluminum-containing adjuvant and the immune response. *Vaccine*, **25,** 6618–6624.

Henke, B.L., Lee, P., Tanaka, T.J., Shamabukruo, R.L., and Fujikawa, B.K. (1982) Low-energy X-ray interaction coefficients: photoabsorption, scattering, and reflection, E =100–2000 eV, Z = 1–94. *Atomic Data & Nuclear Data Tables*, **27**, 1–144

Hsu, P.H. (1967) Effect of salts on the formation of bayerite versus pseudo-boehmite. *Soil Science*, **103**, 101–110.

Hsu, P.H. (1973) Effect of sulfate on the crystallization of aluminum hydroxides from aging hydroxyl-aluminum solutions. Pp. 613–620 in: *Proceedings of the 3rd International Congress on Studies of Bauxites and Aluminum Oxides-hydroxides* (J. Nicolas, editor). Nice, France. ICSOBA, Chambery, France.

Hsu, P.H. (1979) Effect of phosphate and silicate on the crystallization of gibbsite from OH-Al solutions. *Soil Science*, **127**, 219–226.

Hu, Y.F., Boukherroub, R., and Sham, T.K. (2004) Near edge X-ray absorption fine structure spectroscopy of chemically modified porous silicon. *Journal of Electron Spectroscopy & Related Phenomena*, **135**, 143–147.

Hu, Y.F., Zuin, L., Wright, G., Igarashi, R., McKibben, M., Wilson, T., Chen, S.Y., Johnson, T., Maxwell, D., Yates, B.W., Reininger, R., and Sham, T.K. (2007) Commission and performance of the variable line spacing plane grating monochromator beamline at the Canadian Light Source. *Review of Scientific Instruments*, **78**, 083109 (1–5).

Hu, Y.F., Xu, R.K., Dynes, J.J., Blyth, R.I.R., Yu, G., Kozak, L.M., and Huang, P.M. (2008) Coordination nature of aluminum (oxy)hydroxides formed under the influence of tannic acid studied by X-ray absorption spectroscopy. *Geochimica et Cosmochimca Acta*, **72**, 1959–1969.

Huang, P.M. (2004) Soil mineral-organic matter-microorganism interactions: fundamentals and impacts. *Advances in Agronomy*, **82**, 391–472.

Huang, P.M. (2008) Impacts of physicochemical-biological interactions on metal and metalloid transformations in soils: an overview. Pp. 3–52 in: *Biophysico-chemical Processes of Heavy Metals and Metalloids in Soil Environments* (A. Violante, P.M. Huang, and G.M. Gadd, editors). Vol. 1, Wiley-IUPAC series on Biophysico-chemical Processes in Environmental Systems. John Wiley & Sons, Hoboken, NJ, USA.

Huang, P.M. and Violante, A. (1986) Influence of organic acids on crystallization and surface properties of precipitation products of aluminum. Pp. 159–221 in: *Interactions of Soil Minerals with Natural Organics and Microbes* (P.M. Huang and M. Schnitzer, editors). SSSA Special Publication, **17**. Soil Science Society of America, Madison, Wisconsin.

Huang, P.M., Wang, T.S.C., Wang, M.K., Wu, M.H., and Hsu, N.W. (1977) Retention of phenolic acids by non-crystalline hydroxy-aluminum and iron compounds and clay minerals in soils. *Soil Science*, **123**, 213–219.

Huang, P.M., Wang, M.K., Kampe, N., and Schulze, D.G. (2002) Aluminum hydroxides. Pp. 261–289 in: *Soil Mineralogy with Environmental Applications* (J.B. Dixon and D.G. Schulze, editors). SSSA Book Series, no.7. Soil Science Society of America, Madison Wisconsin.

Ildefonse, Ph., Cabaret, D., Sainctavit, Ph., Calas, G., Flank, A.-M., and Lagarde, P. (1998) Aluminium X-ray absorption near edge structure in model compounds and earth's surface minerals. *Physics and Chemistry of Minerals*, **25**, 112–121.

International Centre for Diffraction Data (2007) *Powder Diffraction File™. Alphabetical Indexes for Experimental Patterns. Inorganic Phases.* Sets 1–57. International Centre for Diffraction Data, Newton Square, Philadelphia.

Jiang, N., Qiu, J., and Spence, J.C.H. (2002) Long-range structural fluctuations in a CaO-Al_2O_3-$2SiO_2$ glass observed by spatially resolved near-edge spectroscopy. *Physical Review B*, **66**, 054203(1–5).

Jiang, N. and Spence, J.C.H. (2006) Interpretation of oxygen K- pre-edge peak in complex oxides. *Ultramicroscopy*, **106**, 215–219.

Kasrai, M., Lennard, W.N., Brunner, R.M., Bancroft, G.M., Bardwell, J.A., and Tan, K.H. (1996) Sampling depth of total electron and fluorescence measurements in Si L- and K-edge absorption spectroscopy. *Applied Surface Science*, **99**, 303–312.

Kato, Y., Shimizu, K-I., Matsushita, N., Yoshida, T., Yoshida, A.S., and Hattori, T. (2001) Quantification of aluminum coordinations in alumina and silica-alumina by Al K-edge XANES. *Physical Chemistry Chemical Physics*, **3**, 1925–1929.

Kwong, K.F.N.K. and Huang, P.M. (1975) Influence of citric acid on the crystallization of Al precipitation products. *Clays and Clay Minerals*, **23**, 164–165.

Kwong, K.F.N.K. and Huang, P.M. (1978) Sorption of phosphate by hydrolytic products of aluminum. *Nature*, **271**, 336–338.

Kwong, K.F.N.K. and Huang, P.M. (1979) The relative influence of low-molecular-weight, complexing organic acids on the hydrolysis and precipitation of aluminum. *Soil Science*, **128**, 337–342.

Levesque, P.M., Foster, K., and de Alwis, U. (2006) Association between immunogenicity and adsorption of a recombinant *Streptococcus pneumoniae* vaccine antigen by an aluminum adjuvant. *Human Vaccine*, **2**, 74–77.

Li, D., Bancroft, G.M., Fleet, M.E., Feng, X.H., and Pan, Y. (1995) Al K-edge XANES spectra of aluminosilicate minerals. *American Mineralogist*, **80**, 432–440.

Ma, C.C., Zhou, X., Xu, X., and Zhu, T. (2001) Synthesis and thermal decomposition of ammonium aluminum carbonate hydroxide. *Materials Chemistry and Physics*, **72**, 372–379.

Ogata, F., Kawasaki, N., Nakamura, T., and Tanada, S. (2006) Removal of arsenious ion by calcined aluminum oxyhydroxide (boehmite). *Journal of Colloid and Interface Science*, **300**, 88–93.

Regier, T., Paulson, J., Wright, G., Coulthard, I., Tan, K., Sham, T.K., and Blyth, R.I.R. (2007) Commissioning of the spherical grating monochromator soft X-ray spectroscopy beamline at the Canadian Light Source. *AIP Conference Proceedings*, **879**, 473–476.

Serna, C.J., White, J.L., and Hem, S.L. (1977) Anion-aluminum hydroxide gel interactions. *Soil Science Society*

https://doi.org/10.1346/CCMN.2009.05706012 Published online by Cambridge University Press

of America Journal, **41**, 1009–1013.

Serna, C.J., White, J.L., and Hem, S.L. (1978a) Structural survey of carbonate-containing antacids. *Journal of Pharmaceutical Sciences*, **67**, 324–327.

Serna, C.J., White, J.L., and Hem, S.L. (1978b) Nature of amorphous aluminum hydroxylcarbonate. *Journal of Pharmaceutical Sciences*, **67**, 1144–1147.

Sposito, G. (1996) *The Environmental Chemistry of Aluminum*, 2nd edition. CRC Press, Boca Raton, Florida, 464 pp.

Stohr, J. (1992) *NEXAFS Spectroscopy.* Springer, New York, USA

Tanada, S., Kabayama, M., Kawasaki, N., Sakiyama, T.N., Araki, M., and Tamura, T. (2003) Removal of phosphate by aluminum oxide hydroxide. *Journal of Colloid and Interface Science*, **257**, 135–140.

Thomas, S. and Sherwood, P.M.A. (1992) Valence band spectra of aluminum oxides, hydroxides, and oxyhydroxides interpreted by X_α calculations. *Analytical Chemistry*, **64**, 2488–2495.

van Bokhover, J.A., Sambe, H., Ramaker, D.E., and Koningsberger, D.C. (1999) Al K-edge near-edge X-ray absorption fine structure (NEXAFS) study on the coordination structure of aluminum in minerals and Y zeolites. *Journal of Physical Chemistry B*, **103**, 7557–7564.

van der Marel, H.W. and Beutelspacher, H. (1976) Aluminum minerals. Pp 194–233 in: *Atlas of Infrared Spectroscopy of Clay Minerals and their Admixtures* (H.W. van der Marel and H. Beutelspacher, editors). Elsevier, Amsterdam.

Violante, A. and Huang, P.M. (1985) Influence of inorganic and organic ligands on the formation of aluminum hydroxides and oxyhydroxides. *Clays and Clay Minerals*, **33**, 181–192.

Violante, A. and Huang, P.M. (1993) Formation mechanism of aluminum hydroxide polymorphs. *Clays and Clay Minerals*, **41**, 590–597.

Violante, A., Krishnamurti, G.S.R., and Huang, P.M. (2002) Impacts of organic substances on the formation and transformation of metal oxides in soil environments. Pp. 133–171 in: *Interactions between Soil Particles and Microorganisms* (P.M. Huang, J.M. Bollag, and N. Senesi, editors). Vol. 8, IUPAC series on Analytical and Physical Chemistry of Environmental Systems. John Wiley & Sons, Chichester, UK.

Wang, D. and Anderson, D.W. (1998) Direct measurement of organic carbon in soils by the Leco 12 Carbon Analyzer. *Communications in Soil Science and Plant Analysis*, **29**, 15–21.

Wang, H.M. and Henderson, G.S. (2004) Investigation of coordination number in silicate and germanate glasses using O K-edge X-ray absorption spectroscopy. *Chemical Geology*, **213**, 17–30.

Weigel, C., Calas, I.G., Cornier, L., Galoisy, I.L., and Henderson, G.S. (2008) High resolution Al $L_{2,3}$-edge XANES spectra of Al-containing crystals and glasses: coordination number and bonding information from edge components. *Journal of Physics C*, **20**, 135219 (1–8).

White, W.B. (1974) The carbonate minerals. Pp. 227–284 in: *The Infrared Spectra of Minerals* (V.C. Farmer, editor). Monograph **4**, Mineralogical Society, London.

Yoon, T.H., Hohnson, S.B., Benzerara, K., Dole, C.S., Tyliszczak, T., Shuh, D.K., and Brown, G.B., Jr. (2004) In situ characterization of aluminum-containing mineral-microorganism aqueous suspensions using scanning transmission X-ray microscopy. *Langmuir*, **23**, 10361–10366.

Yu, G., Saha, U.K., Kozak, L.M., and Huang, P.M. (2007) Combined effects of tannate and ageing on structural and surface properties of aluminum precipitates. *Clays and Clay Minerals*, **55**, 369–379.

Zou, Z., Hu, Y.F., Sham, T.K., Huang, H.H., Xu, G.Q., Seet, C.S., and Chan, L. (1999) XAFS studies of Al/TiN_x films on Si(100) at the Al K- and $L_{3,2}$-edge. *Journal of Synchrotron Radiation*, **6**, 524–525.

(*Received 28 August 2008; revised 1 August 2009; Ms. 193; A.E. P. Malla*)

https://doi.org/10.1346/CCMN.2009.05706012 Published online by Cambridge University Press